Intrinsic Structural Distortions in Five-Coordinate (Nitrosyl)iron(II) Porphyrinate Derivatives

W. Robert Scheidt,* Hugues F. Duval, Teresa J. Neal, and Mary K. Ellison

Contribution from the Department of Chemistry and Biochemistry, University of Notre Dame, Notre Dame, Indiana 46556

Received November 12, 1999

Abstract: The preparation and molecular structures of several five-coordinate (nitrosyl)iron(II) porphyrinate derivatives are described. The derivatives reported include two crystalline forms of [Fe(OEP)(NO)] (OEP = 2,3,7,8,12,13,17,18-octaethylporphyrin dianion), three conformationally distinct forms of [Fe(TPPBr$_4$)(NO)] (TPPBr$_4$ = 2,3,12,13-tetrabromo-5,10,15,20-tetraphenylporphyrin dianion), and [Fe(oxoOEC)(NO)] (oxoOEC = 3,3,7,8,12,13,17,18-octaethyl-3*H*-porphin-2-onato(2-) dianion). These complexes differ in the nature and position of the β-pyrrolic and meso substituents, and in the conformation adopted by the porphyrinato cores in the crystalline state. For one form of [Fe(OEP)(NO)], the structure was determined at three temperatures (130(2), 213(2), and 293(2) K). For two of the structures the X-ray data were collected to exceedingly high resolution. For each structure, we observed a bent FeNO group (Fe−N−O angles ranging from 142.74(8)° to 147.9(8)°) and a significant off-axis tilt of the nitrosyl group irrespective of the nature and the conformation of the macrocycle. The tilt of the Fe−N(NO) vector from the heme normal ranges from 5.6 to 8.2°. In all cases, the off-axis tilt of the nitrosyl has an effect on the equatorial Fe−N$_p$ bond distances, leading to an asymmetric interaction of the iron atom with the porphyrinato nitrogen atoms. The structural distortion in the strongly bonding axial nitrosyl ligand appears to be intrinsic and supported only by bonding effects. The presence of a tilt/asymmetry in all ordered five-coordinate (nitrosyl)iron(II) porphyrinate derivatives strongly supports this as an intrinsic structural feature of the total bonding interaction in the five-coordinate complex.

Introduction

The nature of nitric oxide (NO) ligation in hemes has received renewed interest because of the recognition of the participation of NO in a wide variety of biological functions.[1] Although important biological targets of NO are iron porphyrinate derivatives, surprisingly, until very recently, there were no ordered crystal structures of five-coordinate [Fe(Porph)(NO)][2] complexes reported in the literature. The accuracy of the derived coordination group parameters of the few reported species is severely limited by the disorder.[3−5] However, we recently found, in two ordered crystalline polymorphs of the five-coordinate (nitrosyl)iron(II) porphyrinate derivative [Fe(OEP)(NO)],[6] that the FeN$_5$ coordination group shows substantial deviation from the expected axial symmetry. The deviations are a significant off-axis tilt of the Fe−N(NO) bond vector and an apparently correlated asymmetry in the equatorial Fe−N$_p$ bond distances. This equatorial asymmetry pattern is that the two Fe−N$_p$ bonds closest to the tilted Fe−N(NO) axial vector are effectively identical but significantly shorter than the other two Fe−N$_p$ bonds, which are also effectively equal. Hints of deviations from axial symmetry are seen in the disordered five-coordinate (nitrosyl)iron(II) porphyrinate structures,[3−5] and a similar tilting/asymmetry pattern was also present in the structure of a related, recently reported complex.[7] The tilting/asymmetry pattern has also been observed in a cobalt system, although the deviations from ideal axial symmetry are smaller.[8]

That the off-axis tilt and concomitant equatorial bonding asymmetry are observed in the three five-coordinate structures that have adequate accuracy to deal with the issue suggests that tilt/asymmetry in the coordination group could be a hitherto unrecognized, fundamental property of five-coordinate (nitrosyl)-iron(II) porphyrinate derivatives. The experimental data for the two [Fe(OEP)(NO)] derivatives are consistent with a distortion supported only by bonding effects. Accordingly, we have attempted to further characterize the effect. Part of our approach has been to prepare and investigate five-coordinate (nitrosyl)-iron(II) porphyrinate derivatives that vary in the nature and the position of the β-pyrrolic and meso substituents. These derivatives have reduced porphyrin core symmetry and vary in the basicity of the pyrroles. The new complexes studied are derivatives of a β-oxochlorin and the asymmetrically substituted 2,3,12,13-tetrabromo-5,10,15,20-tetraphenylporphyrin. We have

* To whom correspondence should be addressed. Fax: (219) 631-4044. E-mail: Scheidt.1@nd.edu.

(1) (a) Stamler, J. S.; Singel, S. J.; Loscalzo, J. *Science* **1992**, *258*, 1898. (b) Traylor, T. G.; Sharma, V. J. *Biochemistry* **1992**, *31*, 2847.

(2) Abbreviations used in this paper: Porph, a generalized porphyrin dianion; OBTPP, dianion of 2,3,7,8,12,13,17,18-octabromo-5,10,15,20-tetraphenylporphyrin; OEP, dianion of 2,3,7,8,12,13,17,18-octaethylporphyrin; OETAP, dianion of 2,3,7,8,12,13,17,18-octaethyl-5,10,15,20-tetraazaporphyrin; oxoOEC, dianion of 3,3,7,8,12,13,17,18-octaethyl-(3*H*)-porphyrin-2-onato(2−); dioxoOEiBC; dianion of 3,3,8,8,12,13,17,18-octaethyl-(3*H*,8*H*)-porphin-2,7-dionato; trioxoOEHP, dianion of 3,3,7,8,12,12,-18,18-octaethyl-(3*H*,12*H*,18*H*)-porphin-2,13,17-trionato; TPP, dianion of 5,-10,15,20-tetraphenylporphyrin; TPPBr$_4$, dianion of 2,3,12,13-tetrabromo-5,10,15,20-tetraphenylporphyrin; TDCPP, dianion of 5,10,15,20-tetra-2,6-dichlorophenylporphyrin; TpivPP, dianion of 5,10,15,20-α,α,α,α-tetrakis-*o*-pivalamidophenylporphyrin; N$_p$, porphyrinato nitrogens.

(3) Scheidt, W. R.; Frisse, M. E. *J. Am. Chem. Soc.* **1975**, *97*, 17.

(4) Bohle, D. S.; Hung, C.-H. *J. Am. Chem. Soc.* **1995**, *117*, 9584.

(5) Nasri, H.; Haller, K. J.; Wang, Y.; Huynh, B. H.; Scheidt, W. R. *Inorg. Chem.* **1992**, *31*, 3459.

(6) Ellison, M. K.; Scheidt, W. R. *J. Am. Chem. Soc.* **1997**, *119*, 7404.

(7) Bohle, D. S.; Debrunner, P.; Fitzgerald, J.; Hansert, B.; Hung, C.-H.; Thompson, A. J. *J. Chem. Soc., Chem. Commun.* **1997**, 91.

(8) Ellison, M. K.; Scheidt, W. R. *Inorg. Chem.* **1998**, *37*, 382.

10.1021/ja993995y CCC: $19.00
Published on Web 05/02/2000

obtained two crystalline forms of the latter porphyrin which provide derivatives with widely differing core conformations in the solid state. The structural features found in all derivatives are in general accord with the tilt/asymmetry pattern communicated earlier.[6] We report the detailed structural parameters for these new derivatives and describe the final parameters for two solid-state forms of [Fe(OEP)(NO)]. On the basis of the bonding formalism suggested by Enemark and Feltham,[9] and Hoffmann et al.,[10] we have also rationalized the tilt/asymmetry pattern and the bending of the nitrosyl group in terms of a very simple molecular orbital interaction picture.

Experimental Section

General Information. All manipulations involving the addition of NO were carried out under argon using a double-manifold vacuum line, Schlenkware, and cannula techniques. Chloroform, hexanes, methanol, and pyridine were distilled over CaH_2, sodium benzophenone, Mg, and CaH_2, respectively. 2-Methylimidazole was recrystallized from toluene/MeOH, and 1-methylimidazole was distilled under vacuum. NO gas was purified by passing it through 4A molecular sieves immersed in a dry-ice/ethanol slush bath to remove higher oxides of nitrogen.[11] H_2(OEP) was purchased from Midcentury Chemicals, and its iron(III) chloro and perchlorate derivatives were synthesized by modified literature methods.[12,13] *Caution! Although we have experienced no problem with the procedures described in dealing with systems containing the perchlorate ion, they can detonate spontaneously and should be handled only in small quantities; in no case should such a system be heated above 30 °C, and other safety precautions are also warranted.*[14] $H_2(TPPBr_4)$,[15] H_2(oxoOEC),[16] and their (chloro)iron(III) derivatives were also prepared by modified literature methods.[12,13] UV−vis spectra were recorded on a Perkin-Elmer Lambda 19 spectrometer and IR spectra on a Perkin-Elmer model 883 as KBr pellets and/or Nujol mulls. EPR spectra were recorded at 77 K with an X-band Varian E-12 spectrometer. Frozen-solution spectra were obtained in toluene or chloroform.

Preparation of [Fe(OEP)(NO)]. Form A. [Fe(OEP)($OClO_3$)] (30 mg (0.042 mmol)) was dissolved in ~3 mL of $CHCl_3$. To this solution was added 0.5 mL of 0.088 M 2-methylimidazole solution in $CHCl_3$. NO was bubbled into the solution for 10 min. A 1:1 mixture of hexanes and $CHCl_3$ was used as the nonsolvent in the vapor diffusion experiment under a NO atmosphere to obtain X-ray-quality crystals of [Fe(OEP)(NO)](**A**). IR of [Fe(OEP)(NO)](**A**) (Nujol, CH_2Cl_2): ν(NO) = 1666, 1665 cm^{-1}.

Form B. X-ray quality crystals of a second crystalline form, [Fe(OEP)(NO)](**B**), were prepared by reductive nitrosylation of [Fe(OEP)(Cl)] in $CHCl_3$ followed by liquid diffusion using methanol as the nonsolvent.[3] IR of [Fe(OEP)(NO)](**B**) (Nujol, CH_2Cl_2): ν(NO) = 1673, 1665 cm^{-1}. UV-vis (CH_2Cl_2, λ, nm): 389 (Soret), 479, 529, 554.[17,18]

Preparation of [Fe(TPPBr$_4$)(NO)]. Form A. [Fe(TPPBr$_4$)(Cl)] (7 mg (0.007 mmol)) was dissolved in ~3 mL of $CHCl_3$ and 0.1 mL of MeOH. NO was bubbled into the solution for 20 min. Following this reaction, X-ray-quality crystals of [Fe(TPPBr$_4$)(NO)](**A**) were prepared by liquid diffusion using methanol as the nonsolvent. IR of [Fe(TPPBr$_4$)(NO)](**A**) (Nujol): ν(NO) = 1678 cm^{-1}.

Form B. X-ray-quality crystals of a second crystalline form, [Fe(TPPBr$_4$)(NO)](**B**), were prepared by addition of 0.5 mL of 1-MeIm to a solution of 10 mg of [Fe(TPPBr$_4$)(Cl)] in ~3 mL of $CHCl_3$ and 0.1 mL MeOH, followed by liquid diffusion using methanol as the nonsolvent. IR of [Fe(TPPBr$_4$)(NO)](**B**) (Nujol): ν(NO) = 1681 cm^{-1}.

Preparation of [Fe(oxoOEC)(NO)]. [Fe(oxoOEC)(Cl)] (20 mg (0.032 mmol)) was dissolved in ~4 mL of $CHCl_3$/CH_3OH (5:1, v:v). Dry pyridine (0.025 mL) was added through a syringe, and NO gas was bubbled into the solution for 15 min. X-ray-quality crystals were obtained by using hexanes as the nonsolvent in a vapor diffusion experiment under a NO atmosphere. IR (Nujol): ν(NO) = 1690 cm^{-1}. UV−vis (CH_2Cl_2, λ, nm): 412 (Soret), 489, 581, 624.

X-ray Structure Determinations. All data collections were carried out on a Nonius FAST area-detector diffractometer with a Mo rotating anode source ($\bar{\lambda}$ = 0.710 73 Å), using our methods for small-molecule X-ray data collection.[19] Data collections were carried out at 130(2) K for [Fe(OEP)(NO)](**A**), [Fe(TPPBr$_4$)(NO)](**A**), and [Fe(oxoOEC)(NO)], and at 293(2) K for [Fe(TPPBr$_4$)(NO)](**B**).[20] Crystals of [Fe(OEP)(NO)](**B**) and [Fe(oxoOEC)(NO)] diffracted to a very high scattering angle, and data collections were performed at two detector settings. Appropriate power settings were used to maximize the data collected as well as minimize the number of too intense reflections. The data from the two detector settings were merged to a common scale. For [Fe(OEP)(NO)](**B**), data collections were performed on the same crystal specimen at 130, 213, and 293 K. At each temperature, two θ angle settings were used, again with requisite power setting adjustments, to obtain the maximum number of very high angle data. A modified[21] version of the absorption correction program DIFABS[22] was applied to [Fe(OEP)(NO)](**B**), [Fe(TPPBr$_4$)(NO)](**A** and **B**), and [Fe(oxoOEC)(NO)]. A brief description of crystallographic data is given in Table 1.

All structures were solved using the direct methods program SHELXS;[23] subsequent difference Fourier syntheses led to the location of all remaining non-hydrogen atoms. The structures were refined against F^2 with the program SHELXL,[24] in which all data collected were used including negative intensities. All non-hydrogen atoms were refined anisotropically. Hydrogen atoms were idealized with the standard SHELXL idealization methods. Complete crystallographic details are given in the Supporting Information. In the asymmetric unit of [Fe(TPPBr$_4$)(NO)](**A**) there are two independent half-molecules of [Fe(TPPBr$_4$)(NO)] and one and a half chloroform solvent molecules, which are located on mirror planes. The chloroform molecule containing the C(30), Cl(30), Cl(31), and Cl(32) atoms was treated as a rigid group. For [Fe(OEP)(NO)](**A**) and [Fe(oxoOEC)(NO)], the maximum and minimum electron densities on the final difference Fourier maps were 1.51 e/Å^3 (at 0.65 Å from the atom N(5)) and −1.03 e/Å^3 (at 0.59 Å from the atom Fe(1)), and 1.50 e/Å^3 (at 0.72 Å from the atom N(5)) and −2.00 e/Å^3 (at 0.57 Å from the atom Fe(1)), respectively. These residual difference peaks are the result of the extremely high resolution of the data collected ($3° \le 2\theta \le 89°$). For [Fe(TPPBr$_4$)(NO)](**A** and **B**), the maximum and minimum electron densities on the final difference Fourier maps were 1.15 e/Å^3 (at 1.16 Å from the atom 1Br(b4)) and −1.25 e/Å^3 (at 0.85 Å from the atom 2Br(b1)), and 0.89 e/Å^3 (at 0.82

(9) Enemark, J. H.; Feltham, R. D. *Coord. Chem. Rev.* **1974**, *13*, 339. The topic has been revisited by Enemark; see: Westcott, B. L.; Enemark, J. H. Transition Metal Nitrosyls. In *Inorganic Electronic Structure and Spectroscopy, Volume II: Applications and Case Studies*; Lever, A. B. P., Solomon, E. I., Eds.; Wiley: New York, 1999; pp 403−450.

(10) Hoffmann, R.; Chen, M. M. L.; Elian, M.; Rossi, A. R.; Mingos, D. M. P. *Inorg. Chem.* **1974**, *13*, 2666.

(11) Dodd, R. E.; Robinson, P. L. *Experimental Inorganic Chemistry*, Elsevier: New York, 1957; p 233.

(12) (a) Alder, A. D.; Longo, F. R.; Kampus, F.; Kim, J. *J. Inorg. Nucl. Chem.* **1970**, *32*, 2443. (b) Buchler, J. W. In *Porphyrins and Metalloporphyrins*; Smith, K. M., Ed.; Elsevier Scientific Publishing: Amsterdam, The Netherlands, 1975; Chapter 5.

(13) Dolphin, D. H.; Sams, J. R.; Tsin, T. B. *Inorg. Chem.* **1977**, *16*, 711.

(14) Wolsey, W. C. *J. Chem. Educ.* **1973**, *50*, A335; *Chem. Eng. News* **1983**, *61* (Dec 5), 4; **1963**, *41* (July 8), 47.

(15) (a) Callot, H. J. *Tetrahedron Lett.* **1973**, *50*, 4987. (b) Callot, H. J. *Bull. Soc. Chim. Fr.* **1974**, 1492. (c) Crossley, M. J.; Burn, P. L.; Chew, S. S.; Cuttance, F. B.; Newson, I. A. *J. Chem. Soc., Chem. Commun.* **1991**, 1564. (d) Atkinson, S. T.; Brady, S. P.; James, J. P.; Nolan, K. B. *Pure Appl. Chem.* **1995**, 67, 1109.

(16) (a) Chang, C. K.; Sotiriou, C. *J. Org. Chem.* **1985**, *50*, 4989. (b) Inhoffen, H. H.; Nolte, W. *Liebigs Ann. Chem.* **1969**, *725*, 167.

(17) A complete quantitative spectrum of [Fe(OEP)(NO)] has been given in Figure 6 of ref 18. Complete UV−vis spectra for [Fe(oxoOEC)(NO)] and [Fe(TPPBr$_4$)(NO)] are given in the Supporting Information.

(18) Ellison, M. K.; Scheidt, W. R. *J. Am. Chem. Soc.* **1999**, *121*, 5210.

(19) Scheidt, W. R.; Turoskwa-Tyrk, I. *Inorg. Chem.* **1994**, *33*, 1314.

(20) Diffraction maxima for crystals of [Fe(TTPPBr$_4$)(NO)](**B**) were observed to broaden significantly as the temperature was decreased.

(21) The process is based on an adaptation of the DIFABS[22] logic to the area detector geometry by Karaulov: Karaulov, A. I., School of Chemistry and Applied Chemistry, College of Cardiff, University of Wales, Cardiff CF1 3TB, U.K., personal communication.

(22) Walker, N. P.; Stuart, D. *Acta Crystallogr., Sect. A* **1983**, *A39*, 158.

(23) Sheldrick, G. M. *Acta Crystallogr.* **1990**, *A46*, 467.

(24) Sheldrick, G. M. *J. Appl. Cryst.*, manuscript in preparation.

Table 1. Crystallographic Details for [Fe(OEP)(NO)](**A** and **B**), [Fe(TPPBr$_4$)(NO)](**A** and **B**), and [Fe(oxoOEC)(NO)]

	[Fe(OEP)(NO)](**A**)	[Fe(OEP)(NO)](**B**)	[Fe(TPPBr$_4$)(NO)](**A**)	[Fe(TPPBr$_4$)(NO)](**B**)	[Fe(oxoOEC)(NO)]
empirical formula	$C_{36}H_{44}FeN_5O$	$C_{36}H_{44}FeN_5O$	$C_{44}Br_4FeH_{24}N_5O\cdot1.5(CHCl_3)$	$C_{44}Br_4FeH_{24}N_5O$	$C_{36}H_{44}FeN_5O_2\cdot CHCl_3$
FW	618.61	618.61	1191.71	1014.17	753.98
a, Å	14.950(2)	10.4204(1)	16.750(3)	17.623(4)	8.8435(6)
b, Å	22.36192)	10.5562(7)	15.293(3)	10.522(2)	14.1716(13)
c, Å	9.6966(3)	14.0425(7)	17.608(4)	19.457(4)	15.6651(18)
α, deg		79.830(5)			69.946(12)
β, deg	104.854(5)	89.585(4)	107.77(3)	90.78(3)	83.063(7)
γ, deg		80.264(4)			86.647(11)
V, Å^3	3133.3(4)	1498.10(13)	4294.9(15)	3607.6(12)	1830.4(3)
cryst syst	monoclinic	triclinic	monoclinic	monoclinic	triclinic
space group	$P2_1/c$	$P\bar{1}$	$P2_1/m$	$I2/a$	$P\bar{1}$
Z	4	2	4	4	2
cryst color	dark purple	dark purple	dark blue	dark blue	dark purple
cryst dimens, mm	0.56 × 0.40 × 0.27	0.40 × 0.33 × 0.27	0.50 × 0.07 × 0.04	0.23 × 0.23 × 0.16	0.70 × 0.45 × 0.30
total no. of data collected	22655	44013	31981	10550	53891
temp, K	130	130	130	293	130
no. of unique data	7890 (R_{int} = 0.055)	20616 (R_{int} = 0.045)	10958 (R_{int} = 0.109)	4817 (R_{int} = 0.106)	26043 (R_{int} = 0.084)
no. of unique observed data [$I > 2\sigma(I)$]	6949	17208	6661	2335	18419
goodness of fit (based on F^2)	1.283	1.024	1.042	1.054	1.062
final *R* indices [$I > 2\sigma(I)$]	R1 = 0.0421 wR2 = 0.1515	R1 = 0.0412 wR2 = 0.1059	R1 = 0.0755 wR2 = 0.1878	R1 = 0.0982 wR2 = 0.2538	R1 = 0.0781 wR2 = 0.2082
final *R* indices (all data)	R1 = 0.0523 wR2 = 0.1561	R1 = 0.0535 wR2 = 0.1128	R1 = 0.1204 wR2 = 0.2321	R1 = 0.1474 wR2 = 0.3373	R1 = 0.1082 wR2 = 0.2351

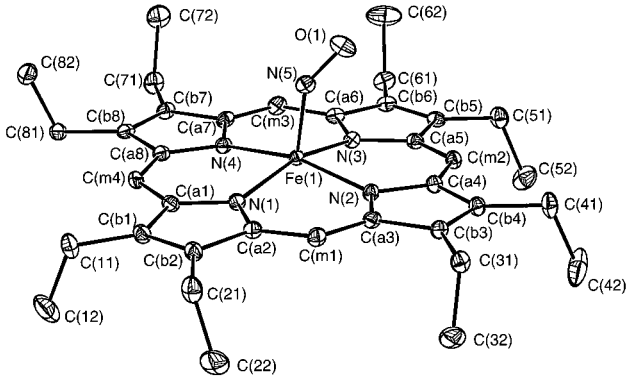

Figure 1. ORTEP diagram of [Fe(OEP)(NO)](**A**) illustrating the tilt of the nitrosyl ligand (50% probability ellipsoids are given). The atom-labeling scheme used in all tables is displayed.

Å from the atom H(b3)) and −1.51 e/Å^3 (at 0.73 Å from the atom Br(b1)), respectively. These residual difference peaks are the result of the anisotropic thermal displacements of the bromo groups.

Results

The molecular and crystal structures of several five-coordinate (nitrosyl)iron(II) derivatives ([Fe(II)(Porph)(NO)]) have been determined; a total of six crystallographically unique structures yielding information about the FeN_4NO coordination group geometry are reported. These include two crystalline polymorphs of [Fe(OEP)(NO)], named [Fe(OEP)(NO)](**A**) and [Fe(OEP)(NO)](**B**). An ORTEP diagram and labeling scheme of [Fe(OEP)(NO)](**A**) is shown in Figure 1. The ORTEP diagram for [Fe(OEP)(NO)](**B**), using the same labeling scheme as for [Fe(OEP)(NO)](**A**), is given in the Supporting Information. In the structure determination of [Fe(TPPBr$_4$)(NO)](**A**), two independent half-molecules of [Fe(TPPBr$_4$)(NO)] were found in the asymmetric unit and are named [Fe(TPPBr$_4$)(NO)](**A′**) and [Fe(TPPBr$_4$)(NO)](**A″**); both metalloporphyrins have required mirror symmetry. The structure of a second crystalline form, [Fe(TPPBr$_4$)(NO)](**B**), is also presented herein. Figure 2 gives ORTEP diagrams of [Fe(TPPBr$_4$)(NO)](**A′** and A″), which also illustrate the labeling schemes for all independent atoms used

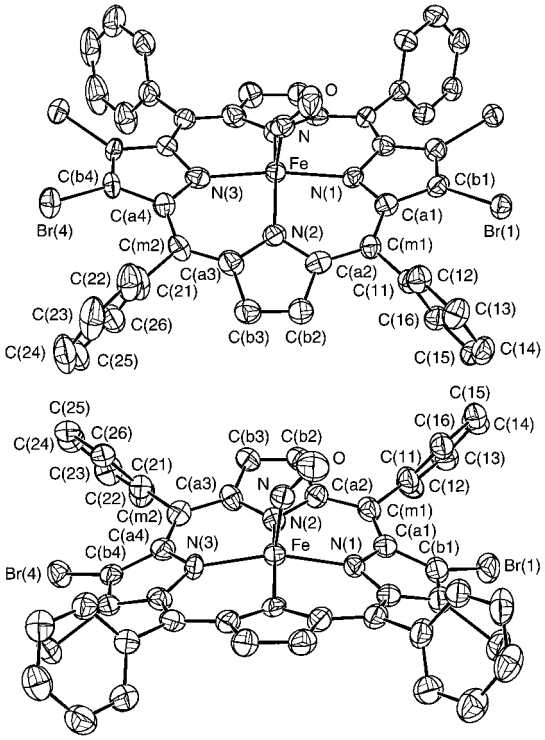

Figure 2. ORTEP diagrams of [Fe(TPPBr$_4$)(NO)](**A′** and **A″**) (top and bottom, respectively) illustrating 50% probability ellipsoids. The crystallographic mirror plane passes through N(1) and N(3). The atom-labeling scheme is used in all tables is displayed.

in the tables. For [Fe(TPPBr$_4$)(NO)](**B**) the ORTEP diagram and the labeling scheme are shown in the Supporting Information. An equivalent illustration for the [Fe(oxoOEC)(NO)] complex is given in Figure 3.

A variety of conformations are adopted by the porphyrinato cores in the five-coordinate {FeNO}^{7} derivatives in the crystalline state. The 24-atom cores of [Fe(OEP)(NO)](**A** and **B**) and [Fe(oxoOEC)(NO)] remain almost planar. For [Fe(TPPBr$_4$)(NO)](**A′**, **A″**, and **B**), there is a strong distortion from planarity that results from the severe crowding between the bulky

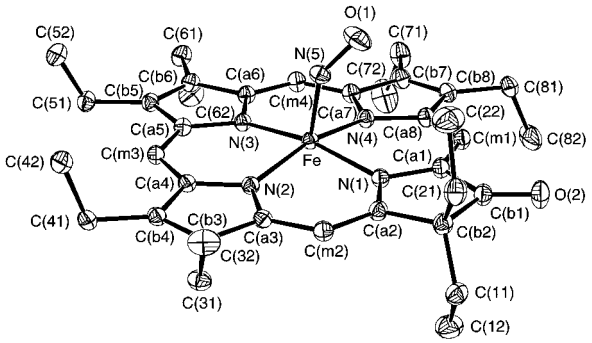

Figure 3. ORTEP diagram of the [Fe(oxoOEC)(NO)] derivative illustrating the overall structure (50% probability ellipsoids). The atom-labeling scheme used in all tables is displayed.

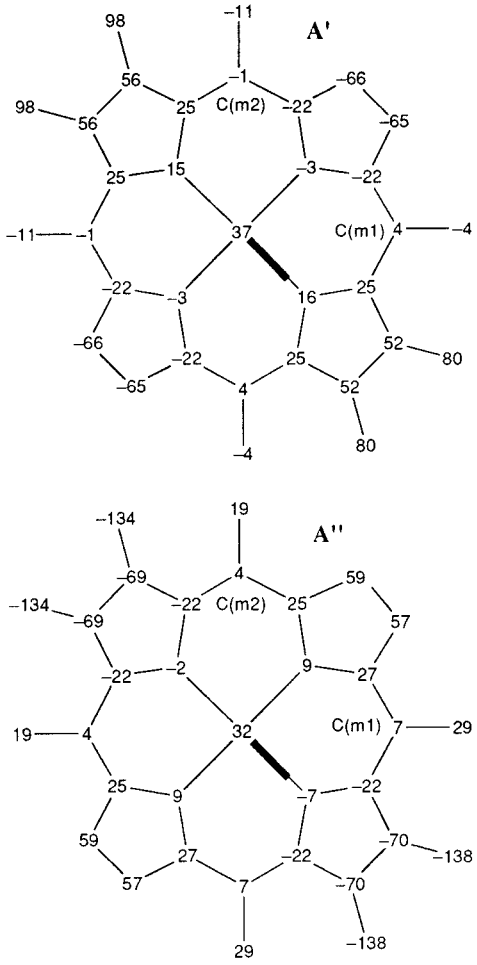

Figure 4. Formal diagrams of the porphyrinato cores of [Fe(TPPBr$_4$)(NO)](**A′**) and [Fe(TPPBr$_4$)(NO)](**A″**) displaying the perpendicular displacements (in units of 0.01 Å) of the porphyrin core atoms, the iron, the bromides, and the first phenyl carbon atoms from the best 24-atom porphyrinato core mean plane.

β-bromide atoms and the phenyl rings. Two of the crystallographically unique structures have strongly saddled porphyrinato cores (**A′** and **A″**, Figure 4), while [Fe(TPPBr$_4$)(NO)](**B**) has a strongly ruffled core.[25]

Tables 2 and 3 display important selected values for the FeN$_4$NO coordination group for the ordered five-coordinate (nitrosyl)iron(II) porphyrin complexes. The Fe−N(NO) bond distance remains relatively constant, ranging from 1.722(2) Å for [Fe(OEP)(NO)](**A**) to 1.734(8) Å for [Fe(TPPBr$_4$)(NO)](**A′**). The N−O bond distance ranges from 1.119(11) to 1.1696(19) Å. Each metalloporphyrin exhibits a bent Fe−N−O group as expected.[9] The bending is effectively constant, ranging from 142.74(8)° for [Fe(OEP)(NO)](**B**) to 147.9(8)° for [Fe(TPPBr$_4$)(NO)](**A′**).

The iron is displaced out of the porphyrinato mean plane in all of these pentacoordinate complexes. The low-spin ground state of these complexes leads to relatively small values of the metal atom displacement from the 24-atom porphyrin cores, ranging from 0.26 Å for [Fe(oxoOEC)(NO)] to 0.37 Å for [Fe(TPPBr$_4$)(NO)](**A′**). The displacements are probably somewhat increased because of steric interactions between the nitrosyl nitrogen atom and atoms of the core and in the case of [Fe(TPPBr$_4$)(NO)](**A′**) because of the saddled core. The dihedral angles between the Fe−N−O plane and the closest Fe−N$_p$ vector are 37.9°, 40.2°, and 40.9°, for [Fe(OEP)(NO)](**A**), [Fe(OEP)(NO)](**B**), and [Fe(oxoOEC)(NO)], respectively. The corresponding dihedral angles are zero for [Fe(TPPBr$_4$)(NO)](**A′** and **A″** (mirror symmetry requirement)), and 18.4° for [Fe(TPPBr$_4$)(NO)](**B**).

Two unusual structural features are observed. First, for each well-ordered crystal structure, the axial Fe−N(NO) vector is not perpendicular to the 24-atom mean plane as might be expected, but is tilted off-axis. The off-axis tilt ranges from 5.6° for [Fe(TPPBr$_4$)(NO)](A′) to 8.2° for [Fe(OEP)(NO)](**B**). This corresponds to a translation of the nitrosyl nitrogen atom off the heme normal of 0.17 Å for [Fe(TPPBr$_4$)(NO)](A′) to 0.25 Å for [Fe(OEP)(NO)](**B**). Second, for each well-ordered crystallographically unique structure, the four equatorial Fe−N$_p$ bonds show a rather large range of values as can be seen in Table 3. These unexpectedly large variations in the equatorial Fe−N$_p$ distances are related to the orientation of the off-axis tilt of the NO. For [Fe(OEP)(NO)](**A** and **B**), the Fe−N$_p$ distances are related in pairs. Two short Fe−N$_p$ distances (averages 1.991(3) and 1.999(1) Å for [Fe(OEP)(NO)](**A**) and [Fe(OEP)(NO)](**B**), respectively) bracket the tilted NO ligand, while two long Fe−N$_p$ distances (averages 2.016(1) and 2.020(4) Å for [Fe(OEP)(NO)](**A**) and [Fe(OEP)(NO)](**B**), respectively) are further from the off-axis NO. The oxochlorin derivative, [Fe(oxoOEC)(NO)], has shorter Fe−N$_p$ bonds (2.0174(13) and 1.9974(12) Å) toward the saturated pyrrole and an adjacent pyrrole ring in the direction of the tilt, and two longer Fe−N$_p$ distances (2.0141(12) and 2.0082(13) Å) in the opposite direction. [Fe(TPPBr$_4$)(NO)](A′ and A″) display two distinctly different saddled conformations in which the NO group tilts toward a brominated pyrrole. The Fe−N−O coordination group and the porphyrinato nitrogen atoms belonging to the disubstituted pyrrole rings lie in a mirror plane in which the Fe−N$_p$ bond distance toward the direction of the tilt is shorter than the opposite one (2.031(8) vs 2.041(9) Å for [Fe(TPPBr$_4$)(NO)](**A′**), and 2.004(7) vs 2.027(7) Å for [Fe(TPPBr$_4$)(NO)](**A″**)). The ruffled TPPBr$_4$ conformer, [Fe(TPPBr$_4$)(NO)](**B**), has a disordered nitrosyl ligand with required 2-fold symmetry; consequently no information about a tilt can be obtained.

For [Fe(OEP)(NO)](**B**), data collections were performed on the same crystal specimen at three different temperatures. The refined off-axis tilt and the translation of the nitrosyl nitrogen from the orthogonal position do not change in any significant way with the change in temperature. A complete listing of coordination group parameters and cell constants for [Fe(OEP)(NO)](**B**) at the three temperatures is given in Table S31 of the Supporting Information.

It is to be noted that the nitrosyl stretching frequencies

(25) Data available in the Supporting Information.

Table 2. Bonding Parameters for [Fe(Porph)(NO)] Complexes

complex	Fe−N−O[a]	ΔFe(Ct)[b,c]	ΔFe(N_4)[b,d]	Fe−N[b]	N−O[b]	orientation[a,e]	tilt[a,f]	ΔN(NO)[b,g]	ref
[Fe(OEP)(NO)](**A**)	144.4(2)	0.29	0.28	1.722(2)	1.167(3)	37.9	6.5	0.19	this work
[Fe(OEP)(NO)](**B**)	142.74(8)	0.27	0.28	1.7307(7)	1.1677(11)	40.2	8.2	0.25	this work
[Fe(TPPBr$_4$)(NO)](**A′**)	147.9(8)	0.37	0.31	1.734(8)	1.119(11)	0.0	5.6	0.17	this work
[Fe(TPPBr$_4$)(NO)](**A″**)	146.9(9)	0.32	0.30	1.726(9)	1.144(12)	0.0	7.1	0.21	this work
[Fe(TPPBr$_4$)(NO)](**B**)	145(1)	0.29	0.28	1.691(11)	1.145(16)	18.4			this work
[Fe(oxoOEC)(NO)]	143.11(15)	0.26	0.26	1.7320(13)	1.1696(19)	40.9	7.1	0.22	this work
[Fe(OETAP)(NO)]	143.7(4)	0.31	*h*	1.721(4)	1.155(5)	39.6	7.6	0.23	7

[a] Value in degrees. [b] Value in angstroms. [c] Iron atom displacement from the 24-atom mean plane. [d] Iron atom displacement from the four nigrogen atom plane. [e] Minimum dihedral angle between the Fe−N−O and N_p−Fe−N(NO) planes. [f] Deviation from the normal to the 24-atom mean plane. [g] Translation of the nitrosyl nitrogen atom off the heme normal. [h] Not reported.

Table 3. Equatorial Fe−N_p Bond Distances (Å)[a]

complex	Fe−N(1)	Fe−N(2)	Fe−N(3)	Fe−N(4)	ref
[Fe(OEP)(NO)](**A**)	**2.016(2)**	*1.989(2)*	*1.993(2)*	**2.017(2)**	this work
[Fe(OEP)(NO)](**B**)	**2.0226(6)**	*2.0000(6)*	*1.9985(6)*	**2.0167(6)**	this work
[Fe(oxoOEC)(NO)]	*2.0174(13)*	**2.0141(12)**	**2.0082(13)**	*1.9974(12)*	this work
[Fe(TPPBr$_4$)(NO)](**A′**)	*2.031(8)*	1.976(5)	**2.041(9)**	*b*	this work
[Fe(TPPBr$_4$)(NO)](**A″**)	*2.004(7)*	1.977(6)	**2.027(7)**	*b*	this work
[Fe(TPPBr$_4$)(NO)](**B**)	1.976(6)	1.926(7)	*c*	*b*	this work
[Fe(OETAP)(NO)]	**1.938**	*1.922*	*1.925*	**1.941**	7

[a] Estimated standard deviations of least significant digits are given in parentheses. The effects of NO tilt on the Fe−N_p bond distances are indicated as follows: those expected to be "long" are indicated in bold type, those expected to be "short" are given in italic type, and those that are not expected to be affected are given in Roman type. [b] Equal to Fe−N(2) by symmetry. [c] Equal to Fe−N(1) by symmetry.

observed (solid state) for the series of new complexes reported here differ little from the ν(NO) frequency range from 1665 to 1705 cm^{-1} reported previously.[3−7] All nitrosyl species exhibited rhombic EPR spectra with hyperfine splitting patterns similar to those reported by Wayland and Olson[26] which are characteristic of five-coordinate iron nitrosyl derivatives. No other EPR signals are apparent.

The synthesis of five new [Fe(Porph)(NO)] derivatives is reported in the Experimental Section. With the exception of [Fe(OEP)(NO)](**A**), all preparations have been reproduced several times. The 2-MeHim and 1-MeHm used in the reported preparations (for [Fe(OEP)(NO)](**A**) and [Fe(TPPBr$_4$)(NO)](**B**), respectively) were in attempts to prepare six-coordinate species.

Discussion

An important issue in nitric oxide complexes is the geometry of the M−N−O group. Early descriptions of the electronic structure of nitric oxide as a ligand emphasized two distinct forms (NO^+ and NO^-) which were associated with linear and bent geometries, respectively. A much preferable formalism for predicting geometry for the metalloporphyrin nitrosyls is the electron-counting formalism suggested by Enemark and Feltham.[9] In this system the NO ligand is not the independent entity that defines the geometry of the complex, but rather the entire MNO group is the independent unit. Thus, the formal oxidation state of the metal ion is always that computed considering the NO ligand as a neutral species, and by extension the porphyrinato dianion will also be first considered as an independent entity. The critical value defining the geometry is the number of electrons in the metal d orbitals plus the number of electrons in the π^* orbitals of NO. The number of electrons is given by n in the notation $\{MNO\}^n$. For nitrosyl metalloporphyrin complexes, which must have square-pyramidal and pseudooctahedral geometries for the five- and six-coordinate derivatives, respectively, the most important values of n are 6, 7, and 8. Experimental metalloporphyrin results show that, for $n = 6$ (e.g., [Mn(TTP)(NO)][27]), MNO is linear, while for $n = 8$ (e.g., [Co(TPP)(NO)][28]), MNO is strongly bent ($\angle$MNO $\approx$ 120°).[29]

All examples of the $\{MNO\}^7$ porphyrinate systems are iron derivatives. Following the conventions above, these could be formally considered iron(II) nitrosyl derivatives. The first structure determined was that of five-coordinate [Fe(TPP)(NO)] in 1975.[3] This was followed by the structures of [Fe(TpivPP)(NO)],[5] [Fe(TDCPP)(NO)],[4] and [Fe(OBTPP)(NO)].[4] All of these structures had a disordered FeN_4NO coordination group which limited the precision of the structural parameters. Nevertheless, these qualitative results allowed some significant conclusions to be drawn. The average Fe−N_p bond distance is 1.99(1) Å, and the average perpendicular displacement of the iron atom from the 24-atom mean plane is 0.29 Å. The average Fe−N(NO) bond distance of 1.720(18) Å remains relatively constant (values range from 1.703(8) to 1.745(61) Å). Although there were large uncertainties in the value of the Fe−N−O angle, the crystallographic results suggest a value in the range of 142−150°. The averaged values for these structural parameters are distinctly different from those seen in the $\{MNO\}^6$ and $\{MNO\}^8$ systems: the M−N(NO) distances, metal ion displacements, and M−N−O angles in the $\{FeNO\}^7$ systems are all intermediate to those observed for analogous species with one fewer and one more electron.

Recently, we were able to determine the extremely precise structure of the five-coordinate derivative [Fe(OEP)(NO)] for two different crystalline forms,[6] obtained from diffraction data collected to very high resolution. The structure of the FeN_4NO coordination group confirmed the general conclusions given above for $\{FeNO\}^7$ systems. More importantly, the high quality of the structural results also revealed unsuspected, subtle stereochemical features around iron that appear to be intrinsic to the $\{FeNO\}^7$ system. The first new feature is an off-axis tilt of the axial Fe−N(NO) vector; i.e., the Fe−N(NO) vectors are several degrees off the heme normal. Second, the equatorial Fe−N_p bond distances showed larger than expected variation for quality structures. We noted that the asymmetry in the equatorial Fe−N_p bonds appeared correlated with the off-axis tilt of the nitrosyl. Our correlation pattern is schematically

(26) Wayland, B. B.; Olson, L. W. *J. Am. Chem. Soc.* **1974**, *96*, 6037.
(27) Scheidt, W. R.; Hatano, K.; Rupprecht, G. A.; Piciulo, P. L. *Inorg. Chem.* **1979**, *18*, 292.
(28) Scheidt, W. R.; Hoard, J. L. *J. Am. Chem. Soc.* **1973**, *95*, 8281.
(29) Scheidt, W. R.; Ellison, M. K. *Acc. Chem. Res.* **1999**, *32*, 350.

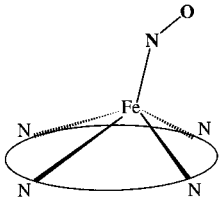

Figure 5. Diagram illustrating the nature of correlated tilt/asymmetry found in five-coordinated [Fe(Porph)(NO)] derivatives. The two equatorial Fe−N_p bonds to the right (in the direction of the tilt) are shortened, while the Fe−N_p bonds to the left are lengthened. The magnitudes of the distortion have been exaggerated for clarity.

depicted in Figure 5, where the significant geometrical features of the two [Fe(OEP)(NO)] species are displayed: the off-axis NO tilt between two pyrrole rings with the Fe−N_p bonds to these two shortened while the remaining two Fe−N_p bonds display a relative lengthening. The conclusion[30] that this tilt and equatorial bond asymmetry are features that are the result of intrinsic bonding effects requires the description of a bonding model. What are the possible details of such a bonding model?

To our knowledge, the issue of an off-axis tilting of coordinated nitric oxide has been addressed only once before. The model involves the critical bonding interaction that leads to the bending of the $\{MNO\}^n$ group (for $n \geq 7$). In this model the important interactions are those of the metal d_{z^2} and d_{xz} orbitals with the π^* orbitals of NO.[10] Hoffmann et al. noted a tilting observed in some square-pyramidal $\{MNO\}^8$ complexes[31,32] and suggested that the tilting resulted from an increased overlap of one π^*_{NO} orbital with the metal d_{z^2} orbital. They suggested that this can be achieved by a sideways movement of the nitrosyl with respect to the normal and which also results in an off-axis tilting. This model is illustrated schematically in Figure 6 (top). However, the direction of the off-axis tilting is opposite to that seen in the (nitrosyl)iron(II) porphyrinates. An alternative way to increase overlap of the π^*_{NO} orbital with the metal d_{z^2} orbital is by a rotation of the metal d_{z^2} orbital with respect to the coordinate frame defined by the porphyrin ligand. This rotation is schematically depicted in Figure 6 (bottom) and must lead to tilting of the NO in the opposite direction of the Hoffmann model. Moreover, the rotation of the d_{z^2} orbital with respect to the basal porphyrin plane (or heme normal) must also lead to small differences in the σ interaction of the metal ion with the basal (porphyrin) ligand when the metal ion is out of the basal porphyrin plane. The basal σ interactions in the direction of the NO (d_{z^2}) tilt will be slightly stronger than those in the direction opposite to the tilt. The model thus rationalizes the observed NO tilt and suggests a clear correlation of equatorial Fe−N_p bond distance asymmetry with the NO tilt direction. Although the model has been applied to five-coordinate (nitrosyl)iron porphyrinate systems, it appears applicable to other square-pyramidal $\{FeNO\}^7$ systems with an apical NO.

We have now prepared and structurally characterized new iron(II) nitrosyls with additional porphyrin ligands to further investigate this tilt/asymmetry and to explore whether it is indeed a general effect. The new porphyrin derivatives are an oxochlorin derivative ([Fe(oxoOEC)(NO)]) and the asymmetrically substituted derivative [Fe(TPPBr$_4$)(NO)], which provides a total

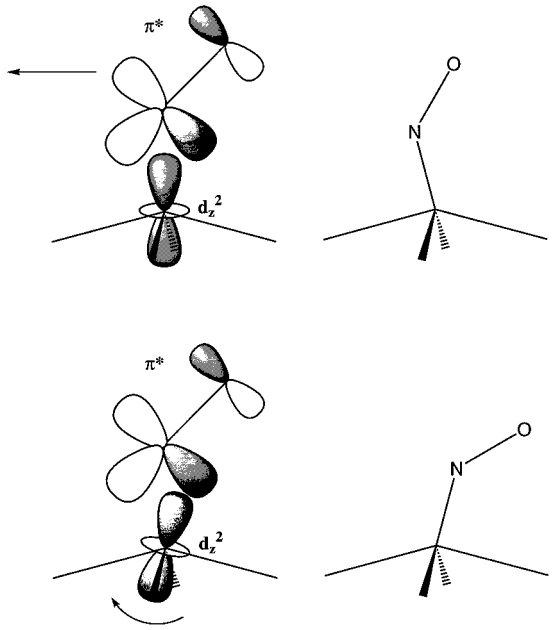

Figure 6. Diagram illustrating possible distortions leading to greater overlap of the half-occupied π^*_{NO} orbital with the iron d_{z^2} orbital that leads to two different tilt directions.

of three independent structures. These two porphyrin derivatives provide species with new patterns for the nature and the position of the β-pyrrolic and meso substituents and in the conformation adopted by the porphyrinato cores in the crystalline state. Although our major concern with the characterization of new derivatives was to obtain ordered structures with sufficient accuracy to address the tilt/asymmetry issues, both of these porphyrin derivatives interact with the central iron atom differently than the OEP derivatives, as described below. Finally, we have also performed multiple-temperature structure determinations for one crystalline form of [Fe(OEP)(NO)] to define any possible temperature effects on the structure. As described in the Results, there is no effect of temperature on the structure. There are thus a total of six well-ordered crystallographically unique nitrosyl structures that are discussed herein.

In the discussion of these structures, we will first deal with the overall stereochemistry and that of the FeNO group, followed by tilt/asymmetry features of the FeN_4NO coordination group. Finally we will discuss conformational issues of the porphyrin macrocycles. As shown in Table 2, the six well-ordered structures exhibit a relatively constant bending of the FeNO group, with the Fe−N−O angle ranging from 142.74(8)° for [Fe(OEP)(NO)](**B**) to 147.9(8)° for [Fe(TPPBr$_4$)(NO)](**A′**). The Fe−N(NO) bond distance is relatively constant, ranging from 1.722(2) Å for [Fe(OEP)(NO)](**A**) to 1.734(8) Å for [Fe(TPPBr$_4$)(NO)](**A′**). The N−O bond distances range from 1.119(11) Å for [Fe(TPPBr$_4$)(NO)](**A′**) to 1.1696(19) Å for [Fe(oxoOEC)(NO)], values consistent with those expected for accurate nitrosyl structures.[29] Other than the possible small effect on the Fe−N−O angle, there is no apparent porphyrin ligand effect on the FeNO group geometry.

All compounds have a low-spin electronic ground state with relatively short Fe−N_p bond lengths that cluster around 2.00 Å, except for the [Fe(TPPBr$_4$)(NO)] derivatives, in which some are slightly longer and will be discussed subsequently. All derivatives have small perpendicular displacements of the iron atom from the 24-atom mean plane of the porphyrin core. Displacements range from 0.26 Å for [Fe(oxoOEC)(NO)] to 0.37 Å for [Fe(TPPBr$_4$)(NO)](**A′**), as shown in Table 2. The

(30) Additional justification for this idea of bonding effects supporting the asymmetry comes for the structure of [Fe(OETAP)(NO)]. We noted that these features are also apparent in the reported structure of [Fe(OETAP)-(NO)].[7]

(31) Mingos, D. M. P.; Ibers, J. A. *Inorg. Chem.* **1971**, *10*, 1035.

(32) Mingos, D. M. P.; Robinson, W. T.; Ibers, J. A. *Inorg. Chem.* **1971**, *10*, 1043.

range of displacement of the iron atom from the nitrogen mean plane is much smaller (Table 2), consistent with the idea that the differing displacement of iron from the porphyrinato core is directly correlated with porphyrin core conformation. In particular, the larger values for the $TPPBr_4$ are the probable result of conformational issues that will be discussed later. The iron displacements are sufficiently small to lead to steric interactions between the nitrosyl nitrogen atom and atoms of the core. The shortest distance between the nitrosyl nitrogen atom and the closest inner nitrogen atom remains essentially short and constant, ranging from 2.68 to 2.74 Å,[25] and can be compared to the sum of the van der Waals radii for nitrogen atoms (3.00 Å). The perpendicular displacement of the N(NO) atom from the four-nitrogen mean plane is constant, ranging from 1.99 to 2.03 Å.

In all of the ordered nitrosyl complexes, there is a deviation from the expected (idealized) structure. The axial Fe−N(NO) vector is not perpendicular to the porphyrin mean plane but is tilted off-axis. The tilt angles range from 5.6° for [Fe($TPPBr_4$)(NO)](**A′**) to 8.2° for [Fe(OEP)(NO)](**B**) (Table 2). This corresponds to a translation of the nitrosyl nitrogen atom off the heme normal (directly correlated with the NO tilt) ranging from 0.17 to 0.25 Å. The determination of the [Fe(OEP)(NO)](**B**) structure at three different temperatures shows no significant differences. The tilt is 7.0° at 293(2) K, 7.8° at 213(2) K, and 8.2° at 130(2) K, and the translation is 0.21, 0.24, and 0.25 Å, respectively. The differences observed are probably caused by thermal foreshortening. No close intermolecular interactions involving NO that might cause the tilting were detected for any of the independent structures. Thus, the off-axis tilt appears to be intrinsic to the FeN_4NO coordination group, is not caused by intermolecular interactions, and is independent of the nature and the geometry of the porphyrinato core.

The last structural feature of the FeN_4NO coordination group is the orientation of the NO ligand with respect to the porphyrin ligand, and the asymmetry in the Fe−N_p bond pattern that is correlated with the tilt/orientation of the NO group. For [Fe(OEP)(NO)](**A** and **B**), [Fe(oxoOEC)(NO)], and [Fe(OETAP)(NO)], the dihedral angle between the Fe−N−O plane and the closest Fe−N_p vector is 37.9°, 40.2°, 40.9°, or 39.6°, respectively. For [Fe($TPPBr_4$)(NO)](**A′** and **A″**), the Fe−N−O group is on the mirror plane that also includes the two N_p atoms of the disubstituted pyrrole rings, and thus the dihedral angle between the Fe−N−O plane and the closest Fe−N_p vector is zero. The orientation in the ruffled, 2-fold disordered [Fe($TPPBr_4$)(NO)](**B**) derivative is 18.4°. The orientation of the NO group for the [Fe($TPPBr_4$)(NO)] derivatives can be understood following an argument first given by Hoffmann et al.[10] They predicted that in square-pyramidal {MNO}^{8} complexes of the type $ML_2L'_2(NO)$, L trans to L, and an axial NO, the nitrosyl group should bend in the plane containing the poorer donors. As the nitrosyl bends, it loses one π interaction, and keeps the stronger one. The better basal donors make the metal a stronger donor in the plane of those donors and the d$\pi-\pi^*$ more stabilizing; this implies bending in the plane of the weaker donors. [Fe($TPPBr_4$)(NO)](**A′** and **A″**) belong to this $ML_2L'_2$(NO) class of complexes albeit with one fewer electron. Due to the electron-withdrawing power of the bromide atoms, the inner nitrogen atoms of the disubstituted pyrrole rings are weaker donors than the other two pyrroles, leading to a bending of the NO group in the plane containing the iron atom and the nitrogen atoms of the two disubstituted pyrrole rings.

The second and most unusual feature occurs in the equatorial Fe−N_p bond pattern. The four equatorial Fe−N_p bonds, for [Fe(OEP)(NO)](**A** and **B**), displayed a rather large spread of values as shown in Table 3. The spread for these two species was subtantially larger than that expected for high-quality structures. The apparent anomaly was resolved when it was recognized that there is a pattern in these distances consistent in both structures. Two short Fe−N_p distances are in the direction of the tilted NO ligand, while two long Fe−N_p distances are opposite the off-axis NO tilt. The averaged short and long distances are 1.991(3) and 2.016(1) Å and 1.999(1) and 2.020(4) Å for [Fe(OEP)(NO)](**A** and **B**), respectively. We also note a similar pattern for [Fe(OETAP)(NO)] (averaged pair distances are 1.924(2) and 1.940(2) Å). The expected long and short pattern is indicated in Table 3, where short bonds are given in italics and long bonds given in bond type.

The new derivatives also display this type of bond distance variation that is correlated with the direction of the nitrosyl tilt. However, there are additional complexities in Fe−N_p bond patterns in the remaining derivatives owing to asymmetry induced by the peripheral substituents. The dihedral angle between the Fe−N−O plane and the closest Fe−N_p vector in [Fe(oxoOEC)(NO)] is 40.9° and is between N(1) and N(4). The Fe−N(NO) vector is tilted off the normal between N(1) and N(4). We would thus expect that the equatorial Fe−N(1) and Fe−N(4) bonds would be the short pair while the Fe−N(2) and Fe−N(3) bonds would be the long pair. Indeed Fe−N(4) is the shortest bond in the complex (Table 3). Fe−N(1) does not appear to follow the pattern as it is the longest bond. However, N(1) is part of the pyrrolinone ring (Figure 3); this is expected to have a significant effect on the Fe−N(1) distance. The pattern is observed in β-oxo species is that there is a "long" M−N_p distance to the pyrrolinone ring and "short" M−N_p distances to the pyrroles. For example, in the [Fe(oxoOEC)(Cl)][33] and [Fe(dioxoOEiBC)(Cl)][34] derivatives the difference between the short Fe−N_p distances and the long Fe−N distances is ∼0.64 Å. This bond distance pattern is also found in all other crystallographically characterized β-oxo species: [Ni(oxoOEC)],[35] [Ni(dioxoOEiBC)],[36] [Ni(trioxoOEHC)],[36] [Cu(oxo)OEC)],[37] [Cu(oxoOEC$^\bullet$)]$SbCl_6$,[37] and [Cu(dioxoOEiBC)].[38] The magnitude of the bond length difference does depend on stereochemical features with smaller differences seen for in-plane metals. Differences range upward from 0.02 Å. Extrapolating to [Fe(oxoOEC)NO)], we would expect a difference ∼0.03 Å between the long and short bonds; the expected difference is larger than that actually observed. We conclude that the off-axis tilt of the NO axial ligand leads to a shortening of Fe−N(1) as well as Fe−N(4), and the pattern similar to that of previously described five-coordinate (nitrosyl)iron(II) porphyrinate derivatives is present.

The two independent molecules of [Fe($TTPBr_4$)(NO)] (**A′** and **A″**) have required crystallographic mirror symmetry with the mirror plane perpendicular to the mean plane of the core and bisecting the pair of brominated pyrrole rings. The mirror also requires that the dihedral angle between the Fe−N−O plane and the closest Fe−N_p vector be 0°. In both molecules the Fe−N−O plane is in the direction of one of the bromo-substituted

(33) Neal, T. J.; Kang, S.-J.; Schulz, C. E.; Scheidt, W. R. *Inorg. Chem.* **2000**, *39*, 872.
(34) Barkigia, K. M.; Chang, C. K.; Fajer, J.; Renner, M. W. *J. Am. Chem. Soc.* **1992**, *114*, 1701.
(35) Stolzenberg, A. M.; Glazer, P. A.; Foxman, B. M. *Inorg. Chem.* **1986**, *25*, 983.
(36) Connick, P. A.; Haller, K. J.; Macor, K. A. *Inorg. Chem.* **1993**, *32*, 3256.
(37) Neal, T. J.; Kang, S.-J.; Schulz, C. E.; Scheidt, W. R. *Inorg. Chem.* **1999**, *38*, 4294.
(38) Chang, C. K.; Barkigia, K. M.; Hanson, L. K.; Fajer, J. *J. Am. Chem. Soc.* **1986**, *108*, 1352.

pyrroles. The N−O bends toward the less basic dibromopyrrole as suggested.[10] The Fe−N(NO) vector is tilted off the normal in this direction and lies in the mirror plane. We would thus expect that only the Fe−N_p bonds lying in the mirror plane would be affected by the NO tilt. As seen in Table 3, this is what is observed, although the differences in the two bond lengths are marginally significant. As will be discussed subsequently, the transannular distance between the bromo-substituted pyrroles is larger than that between the unsubstituted rings as a result of the asymmetric substitution at the periphery. Hence, these average Fe−N_p distances, although affected by the NO tilt, are longer than the average to the unsubstituted pyrroles. The difference in Fe−N_p bond lengths to the brominated pyrrole rings in the two independent half-molecules is a consequence of the differing type of saddling in the two forms (vide infra).

In this final section we consider porphyrin core conformation and the consequent effects of the FeN_4NO coordination group. The porphyrin cores in both OEP forms (**A** and **B**), the oxoOEC derivative, and the OETAP derivative all have β-pyrrole substituents only, there is no peripheral substituent crowding, and the 24-atom cores are essentially planar in the crystalline state. [Fe(OEP)(NO)](**A**) displays an additional very small saddling, and [Fe(oxoOEC)(NO)] shows a small saddling and ruffling that are superimposed on the essential planarity of the macrocycles. The maximal perpendicular displacement of a porphyrinato core atom from the 24-atom mean plane in these derivatives is 0.13 Å (β-pyrrole carbon atom C(b1)) for [Fe(oxoOEC)(NO)].[25]

The $TPPBr_4$ dianion has a very different substitution pattern with four phenyl groups at the meso positions and four bromide atoms at the β-pyrrole positions of two diametrically opposed pyrrole rings. This pattern leads to two trans sets of pyrroles with distinctly different basicities. Additionally, there are very tight nonbonded distances between the β-bromides and the closest carbon atoms of the phenyl rings. These distances are tabulated in Table S32 and range from 3.13 Å upward; the sum of the van der Waals radii for bromide and an aromatic carbon is 3.65 Å. This crowding between the phenyl groups and the bulky peripheral bromides induces both in-plane and out-of-plane distortions of the porphyrinato core.

The in-plane distortion is an elongation of the central porphyrin cavity that leads to unequal transannular N···N distances,[39] with the distances involving the trans-brominated rings larger. Hence, the Fe−N_p distances to the brominated pyrrole ring nitrogen atoms are always larger than the distances to the unsubstituted ring nitrogen atoms. The magnitude of the difference is related to the out-of-plane porphyrinato core distortion, i.e., the core conformation. These conformations are strongly saddled cores for [Fe($TPPBr_4$)(NO)](**A′**and **A″**) and a strongly ruffled core for [Fe($TPPBr_4$)(NO)](**B**).[40,41] The core conformations have interesting effects on the equatorial distances.

The saddled form of [Fe($TPPBr_4$)(NO)] has two distinct conformations of the porphyrinato ring as shown in Chart 1. The two limiting forms can be referenced with respect to the direction of the out-of-plane displacement of the iron atom. In **A′**, the two brominated pyrrole rings are tipped so that the bromine atoms are on the same side of the porphyrin plane as the iron, while in **A″** the two brominated rings are on the opposite side of the iron atom. The extent of the tipping is different in the two conformers. Values of the dihedral angles between trans-brominated pyrrole rings and trans-unsubstituted rings are 21.0 and 34.6°, respectively, in conformer **A′**. The corresponding dihedral angle values in conformer **A″** are 36.1° and 26.1°. The two different conformations result in the two nitrogen atoms of the brominated pyrroles being displaced on the iron side of the 24-atom plane in **A′** and on the opposite side in **A″** (see Figure 4).

Chart 1

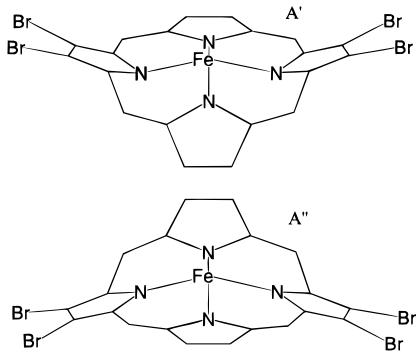

These differences in the relative pyrrole nitrogen atom position would lead to large differences in the values of Fe−N_p if the central hole of the porphyrin retained a constant shape (size). However, the interaction of the central iron has a strong effect, and the shapes of the central hole in the two conformers are significantly different. The Fe−N_p distance to the more basic, unsubstituted pyrroles is the same in the two conformers with a distance of 1.976(5) or 1.977(6) Å, suggesting a constant bonding interaction. The Fe−N_p distances to the brominated rings are also similar in the two conformers with an average distance of 2.036 Å in **A′** and 2.016 Å in **A″**. The near identity of the bonding distances in the two conformers is achieved through significantly different N···N transannular distance pairs. The two distances are 4.049 and 3.871 Å in **A′** and 3.963 and 3.926 Å in **A″**, with the trans-brominated ring distance given first for each pair. The reason for the two types of saddled conformations is not clear, but it is to be noted that the **A′** type of conformer has been observed in [Fe($TPPBr_4$)Cl)],[42] while the **A″** conformer has been found in [Fe($TPPBr_4$)]$_2$O.[43] In these two high-spin derivatives, the N···N transannular distance pair differences show much smaller effects between the two conformations, presumably reflecting the weaker bonding interaction between high-spin iron(III) and the porphyrin ligand. Finally, as can be seen in Figure 4, the first carbon atom of all phenyls is displaced on the side of the porphyrin plane opposite that of the β-bromine substituents.

In our attempts to prepare a six-coordinate derivative of [Fe($TPPBr_4$)(NO)], we isolated a five-coordinate conformer with a ruffled core. The ruffled core in [Fe($TPPBr_4$)(NO)](**B**) should lead to overall shorter equatorial distances while retaining Fe−N_p bond differences between the two ring types. The ruffling, along with the required 2-fold symmetry, leads to Fe−N_p distances of 1.976(6) Å to the brominated pyrrole and 1.926(6) Å to the unsubstituted ring; the relative magnitudes are in accord with the conformation.

(39) Scheidt, W. R. In *The Porphyrin Handbook*; Kadish, K. M., Smith, K., Guilard, R., Eds.; Academic Press: San Diego, CA, and Burlington, MA, 1999; Vol. 3, Chapter 16.

(40) The two conformations both have D_{2d} geometry. In the saddled (*sad*) form, the pyrrole rings are tipped, alternately, above and below the mean plane, while the meso carbon atoms are in the mean plane. In the ruffled (*ruf*) form, the meso carbon atoms are alternatively above and below the mean plane. See ref 41 for further illustration.

(41) Scheidt, W. R.; Lee, Y. *Struct. Bonding (Berlin)* **1987**, *64*, 1.

(42) Duval, H. F.; Bulach, V.; Fischer, J.; Renner, M. W.; Fajer, J.; Weiss, R. *J. Biol. Inorg. Chem.* **1997**, *2*, 662.

(43) Kadish, K. M.; Autret, M.; Zhongping, O.; Tagliatesta, P.; Boschi, T.; Fares, V. *Inorg. Chem.* **1997**, *36*, 204.

The observed off-axis NO tilt may have some effect on the molecular dynamics associated with the rotation of the nitrosyl group. Mason and co-workers[44] have shown by ^{15}N CPMAS NMR spectroscopy that the bent nitrosyl in the cobalt derivative [Co(TPP)(NO)] undergoes a swinging motion in the solid state between four equivalent sites for NO. The asymmetric interaction between iron and its five ligands may be a significant source of the barrier toward such swinging of NO. Since the asymmetry (tilt) is larger in the iron systems than in the one known cobalt case,[8] a rotation barrier higher than that expected from the Mason experiment may exist for the iron nitrosyl case.

Conclusions

The structures for all well-ordered five-coordinated (nitrosyl)-iron(II) porphyrinato derivatives have been presented herein. All data obtained continue to suggest that the FeNO unit should be regarded as the strongly delocalized entity that determines physical and structural properties. Although the assignment of the oxidation state of iron can be made and is preferable to an assignment of NO oxidation state (which is likely to be arbitrary), the $\{FeNO\}^7$ notation that explictly accounts for metal and nitrosyl electrons is preferable. These iron deriatives have a partly bent Fe−N−O group (angle 143−147°) and a Fe−N(NO) bond distance of 1.72−1.74 Å. The compounds studied strongly support the structural feature of tilt/bending of the FeNO group, along with an asymmetry in the equatorial Fe−N_p interactions. These intrinsic features of the total bonding interactions in the complex are independent of the point group symmetry, the nature and position of the β-pyrrolic and meso substituents, and the conformation adopted by the porphyrinato cores in the crystalline state. It is possible to rationalize the tilt/asymmetry feature in terms of bonding molecular orbital interactions. It is yet to be determined whether this tilting leads to any particular reactivity, but the tilting is consistent with the FeNO unit dominating the bonding in the complexes. These $\{FeNO\}^7$ porphyrinate systems are unique; there are no known nitrosyl porphyrin species equivalent to iron(II) based on anoher metal.

(44) Groombridge, C. J.; Larkworthy, L. F.; Mason, J. *Inorg. Chem.* **1993**, *32*, 379.

Acknowledgment. We thank the National Institutes of Health for support of this research under Grant GM-38401. Funds for the purchase of the FAST area-detector diffractometer were provided through NIH Grant RR-06709 to the University of Notre Dame.

Supporting Information Available: Tables S1−S30, giving complete crystallographic details, atomic coordinates, bond distances and angles, anisotropic temperature factors, and fixed hydrogen atom positions for the [Fe(OEP)(NO)](**A**), [Fe(OEP)-(NO)](**B**), [Fe(oxoOEC)(NO] [Fe(TPPBr$_4$)(NO)](**A′** and **A″**), and [Fe(TPPBr$_4$)(NO)](**B**) derivatives; Table S31 listing the coordination group parameters and cell constants of [Fe(OEP)-(NO)](**B**) at three temperatures; Table S32 giving nonbonded contacts in the [Fe(TPPBr$_4$)(NO)](**A′**, **A″**, and **B**) conformers; Figures S1 and S2 showing ORTEP diagrams of [Fe(OEP)-(NO)](**B**) with 50% probability ellipsoids and [Fe(TPPBr$_4$)(NO)]-(**B**) with 30% probability ellipsoids, respectively (the atom-labeling schemes used in all tables are also displayed); Figures S3−S7 displaying the perpendicular displacements (in units of 0.01 Å) of the porphyrin core atoms from the 24-atom mean plane, for [Fe(OEP)(NO)](**A**), [Fe(OEP(NO)](**B**), [Fe(OETAP)-(NO)], [Fe(oxoOEC)(NO)], and [Fe(TPPBr$_4$)(NO)](**B**), respectively; Figure S8-S12 showing the nonbonded contact for the nitrogen of the nitrosyl group, for Fe(OEP)(NO)](**A**), [Fe(OEP)-(NO)] (**B**), Fe(oxoOEC)(NO)], [Fe(TPPBr$_4$)(NO)](**A′**), and [Fe(TPPBr$_4$)NO)](**A″**), respectively; and Figures S13−S14, giving complete UV−vis spectra for [Fe(TPPBr$_4$)(NO)] and [Fe(oxoOEC)(NO)] (PDF, CIF). This material is available free of charge via the Internet at http://pubs.acs.org.

JA993995Y